

# Scan-based near-field acoustical holography on rocket noise

Michael D. Gardner

*N283 ESC Provo, UT 84602*

Scan-based near-field acoustical holography (NAH) shows promise in characterizing rocket noise source regions. A brief explanation of NAH is followed by a description of the virtual coherence technique, which allows one to perform scan-based NAH on uncorrelated fields through the use of multiple stationary reference microphones. Numerical experiments are performed intended to mimic rocket noise with the purpose of determining guidelines for proper number and placement of reference microphones. Results show using more reference microphones is better and proper microphone placement depends upon various factors including frequency and coherence length.

## I. Introduction

Noise generated from rocket boosters presents significant problems to any who are exposed to rocket noise. Field tests done by Brigham Young University students and faculty find that sound pressure levels (SPL) from rocket boosters can approach 190 dB<sub>re 20μPa</sub> a few meters away from the plume. One person<sup>1</sup> measured the total sound power level from a space shuttle solid rocket booster motor to be 196 dB<sub>re 10<sup>-12</sup> W</sub>. To put this in perspective, the threshold of pain for human hearing occurs around 130 dB SPL and a 196 dB sound power level corresponds to 40 MW of sound power. To understand the impact of rocket noise to the surrounding environment and perhaps to mitigate its effect, a better understanding of the noise source region is needed.

Analytical or numerical modeling of rocket noise is quite limited in applicability. This is greatly due to the turbulent nature of the rocket plume. An alternative to modeling rocket noise is to measure it experimentally. Placing microphones directly in the plume is not possible due to the plume's fast mean flow and hot temperature. Instead of placing microphones in the flow region, near-field acoustical holography (NAH) proposes putting the microphones just outside the shear layer of the rocket plume and then reconstructing appropriate acoustical properties (such as pressure and particle velocity) in the source region.

## II. Methods

Near-field acoustical holography involves taking a two-dimensional map of pressure in the near field of some source; this is called the hologram. Using appropriate Green's functions, this hologram can be used to reconstruct the pressure or velocity in the entire three-dimensional field between the source and the hologram. The measurements are made in the near field in order to capture evanescent waves, thus garnering more information about the source radiation characteristics.<sup>2</sup> Figure 1 shows an example of NAH for a planar measurement.

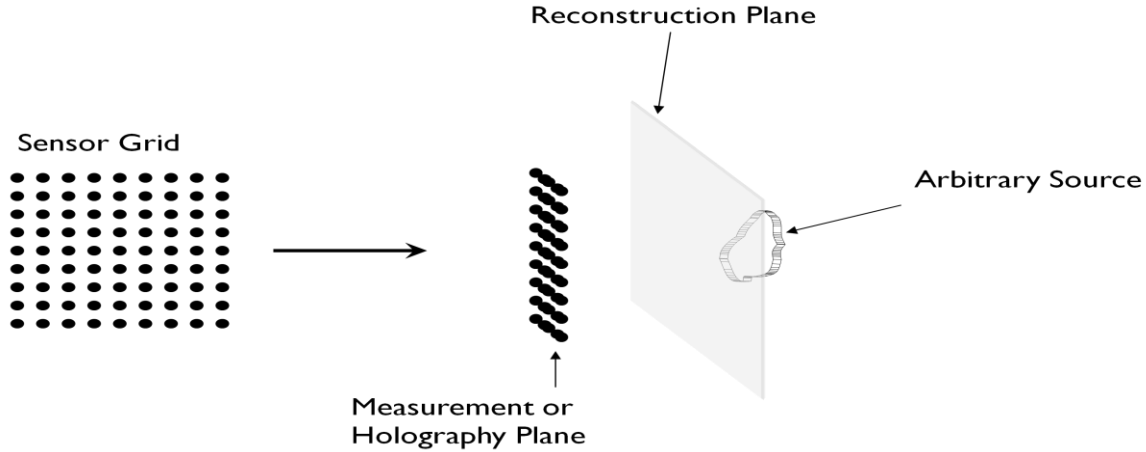


**Figure 1** Diagram showing a typical NAH experimental geometry.

NAH gives more information than other array based methods such as beamforming.<sup>3</sup> NAH requires a coherent field (i.e. fixed phase relationship between measurement points). If all the desired measurement locations are taken simultaneously ("snapshot approach"), this requirement is satisfied. If, however, there are more measurement locations than there are available microphones, a scan-based approach is needed. For a coherent source such as a vibrating plate, a single stationary reference microphone is required to correlate the data across scans. For uncorrelated sources or partially correlated sources, as is the case with rocket noise, the virtual coherence technique<sup>4</sup> allows one to perform scan-based NAH by using multiple stationary reference microphones. This technique decomposes the total sound field into completely coherent, but mutually incoherent partial fields. This technique is also called partial field decomposition. These partial fields can then each be subjected to NAH, which will reconstruct them closer to the source. These reconstructed fields can then be added quadratically to obtain total sound field at the reconstruction locations.

In brief the virtual coherence technique works by decomposing the cross-spectral matrix of the reference microphones,  $C_{rr}$ , via the singular value decomposition as follows:

$$C_{rr} = U\Sigma V^H \quad (1)$$

where  $U$  and  $V$  consist of the left and right singular vectors of  $C_{rr}$ , and  $\Sigma$  is the diagonal matrix of the singular values. The singular values become the autospectral amplitudes of the new virtual references, which are completely independent of one another since there are no off-diagonal terms. With the transformation in Eq. 1, the transfer function  $H_{rp}$  becomes  $H_{vp}$ , which is then used to obtain the partial fields<sup>5</sup>.

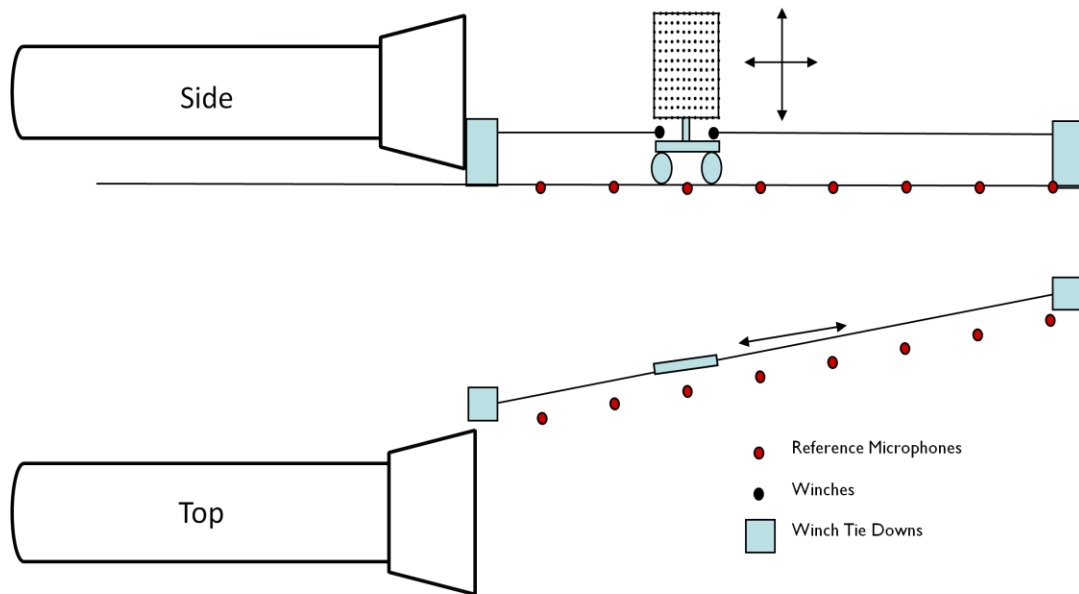


**Figure 2** Hypothetical measurement of rocket booster using scan-based NAH with scan grid and reference microphone locations shown

Shown in Fig. 2 is a diagram of a scan-based NAH measurement on a rocket booster showing the microphone grid being scanned along the shear layer of the plume along with stationary reference microphones. With typical rocket burn times of about 2 minutes, the microphone grid could perhaps be moved from each scan position every 10 seconds, thus increasing the effective measurement grid twelve fold. For good reconstruction resolution at typical frequencies of interest, an exorbitant number (perhaps thousands) of microphones would be required to do a snapshot NAH measurement of a typical rocket plume. In contrast, with only 100 microphones, 1200 measurement locations could be achieved.

Although several people have used NAH in conjunction with the virtual coherence technique<sup>3,5-6</sup>, my research endeavored to establish guidelines for proper number and location of reference microphones for use on a large-scale rocket. The theory of virtual coherence states that one must have as many reference microphones as there are independent sources. More reference microphones is always better, as it amplifies the significant singular values compared to the noise. It is difficult to state how many independent sources exist in a rocket plume because it is a continuous distribution of sources. Only one reference microphone would be required for a continuous source that was perfectly coherent such as a line source (e.g. a vibrating rod). When the source is partially correlated, there is an "effective" number of independent sources which is less than the total number of sources. The coherence length  $L_s$  (Eq. 1) allows one to determine how correlated a source is over distance. The coherence length is used in conjunction with the virtual coherence function to determine an effective number of sources, where the virtual coherence function determines if there are enough partial fields (and thus reference microphones) to effectively represent the field.

Numerical simulations are performed that attempt to mimic the known source characteristics of rockets. These aid in determining proper reference microphone placement. While a detailed numerical model of rocket noise is not in the scope of this research, attempts have been made to be faithful to general aspects of current rocket noise models. For the purposes of these simulations, only the source strengths radiating at 90 degrees to plume axis will be used, meaning only the source mechanisms that radiate omnidirectionally will be simulated. The source region will be treated as a line source of densely spaced monopoles. The amplitude of the sources as a function of frequency will match the observed behavior: higher frequency components closer to the nozzle, and lower frequency components further downstream. Coherence lengths will also match current models: longer lengths for lower frequencies and shorter lengths for higher frequencies. Coherence lengths also increase as the source mechanisms travel downstream, especially for higher frequencies. The coherence lengths or lengthscales are modeled as follows<sup>7</sup>:

$$L_s/D = 1/(1 + 25St) \quad (2)$$

Where  $L_s$  is the lengthscales,  $D$  is the diameter of the nozzle, and  $St$  is the Strouhal number defined as  $St = fD/U$  ( $f$  is frequency and  $U$  is plume exit velocity). Therein lies the frequency dependence of the coherence lengths. For this paper, the coherence length is the distance at which the coherence function between sources has dropped to 0.5.

### III. Results

A numerical experiment was performed with 100 sources spaced from 0 to 50 meters downstream of the hypothetical rocket nozzle. The two frequencies looked at for this case were 20 Hz and 100 Hz. The plume exit velocity  $U$  was chosen to 2600 m/s, or mach 7.6,  $D$  is 3.7 meters, and thus the coherence lengths for the frequencies were chosen appropriately to match Eq. 2. Figure 3 shows the setup of the numerical experiment. The scanning grid had 25 microphones in it, 5 in the vertical direction and 5 in the horizontal direction. The grid was scanned 11 times horizontally down the plume starting at 4 meters before the first source and ending at the last source, 50 meters downstream. The scanning plane was 2 meters away from the line array of sources and the reconstruction plane was 0.3 meters away. Thirty-six stationary reference microphones were used in two cases: one in which they were linearly spaced from the nozzle to the last source, and one in which they were logarithmically spaced, with the more densely spaced region closer to the nozzle. The idea behind this is that more closely spaced reference microphones should be put in regions of high frequency and low coherence length, to best capture the rapidly varying nature of the field.

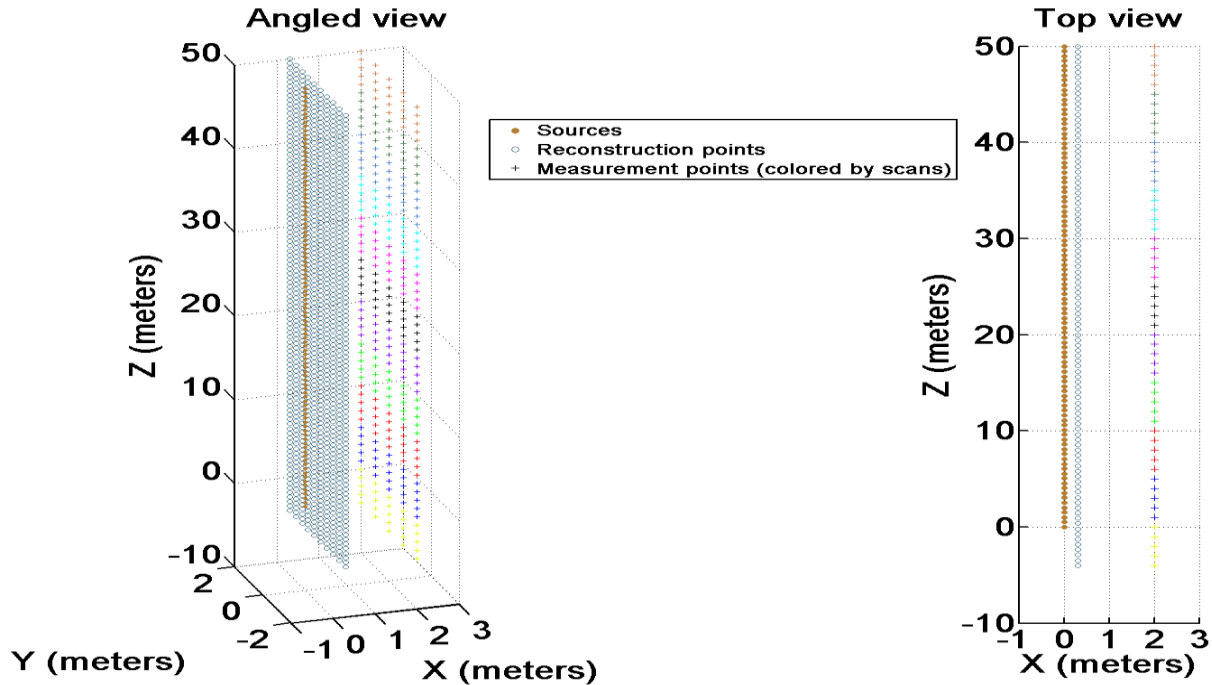


**Figure 3** The numerical experiment geometry showing an angled view (left) of the sources, reconstruction points, and measurement points, and a top view (right).

All the processing was done in the frequency domain. Normally distributed random complex amplitudes were generated for all the 100 sources for each of the 11 scans, 51 blocks per scan.

The free space Green's function,  $\frac{e^{-jkr}}{r}$  ( $k$  is the wavenumber and  $r$  is the distance from the source), was used to propagate the pressures out to the measurement points and the reconstruction points for the benchmark. Partial field decomposition was then performed to obtain the partial fields from the measurement pressures and reference pressures. The partial fields were then sent to be processed by Statistically Optimized NAH<sup>8</sup> (SONAH) in planar coordinates which reconstructed the fields at the reconstruction plane 0.3 meters away from the sources (see Fig. 3). SONAH was used because of its flexibility in measurement geometry and because it eliminates a lot of spatial windowing effects in comparison with other NAH methods. The reconstructed fields are then summed on a quadratic basis to obtain a pressure magnitude plot at the reconstruction surface.

The measured pressure across the scans at 100 Hz is shown in Fig. 4. The actual dB scale of all the figures in this paper is irrelevant since it is only the relative amplitudes that are important for NAH. The field is choppy across scans due the uncorrelated nature of the source. The virtual coherence technique is used on the field and the final reconstructed pressure along with the benchmark is shown in Fig. 5. The RMS error between the benchmark and the reconstruction is 4.2 dB. This result uses reference microphones spaced linearly along the source region as shown in Fig. 6. The dB pressures are compared on the horizontal line that is in the vertical center of

the array in the bottom of Fig. 6. This shows the agreement is quite good in the hot region and overestimates the pressure at the ends of the full scan. The top half of Fig. 6 also shows the coherence length as a function of distance downstream.

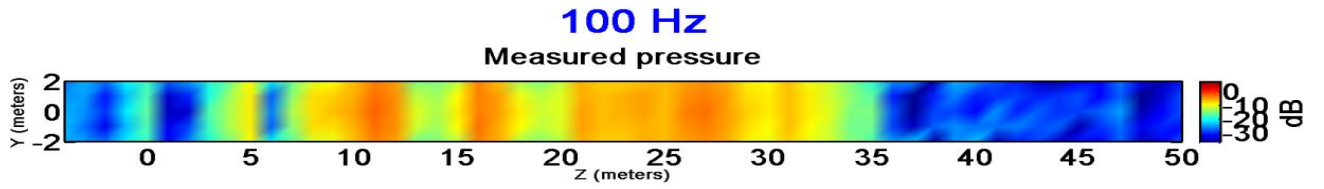


Figure 4 Measured pressure (dB) at 100 Hz for all the scan positions averaged over blocks

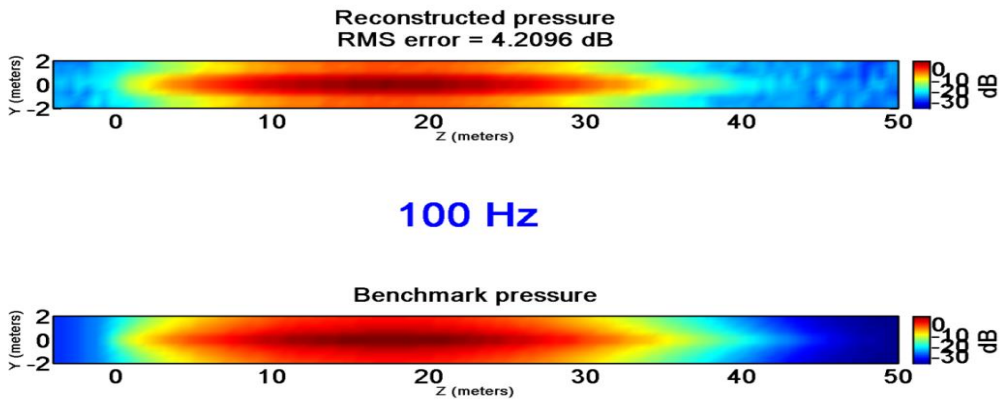
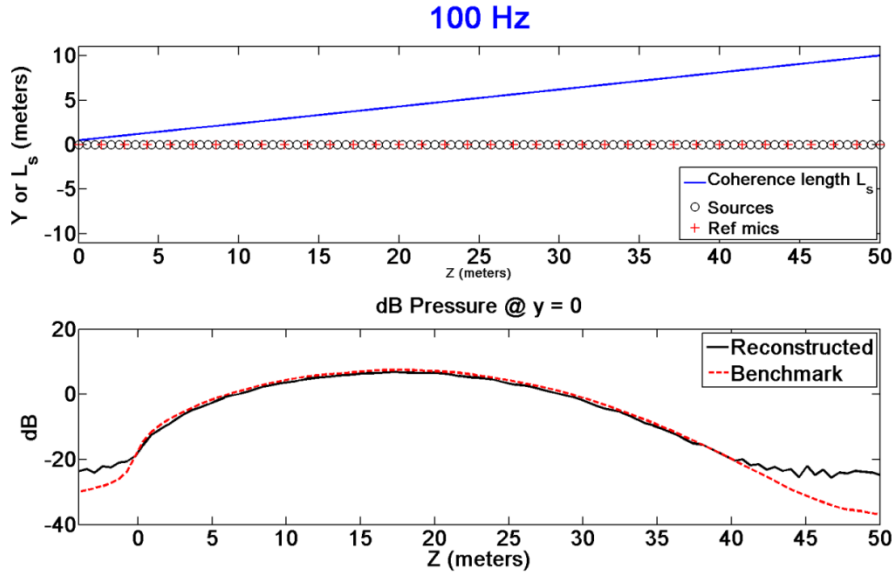
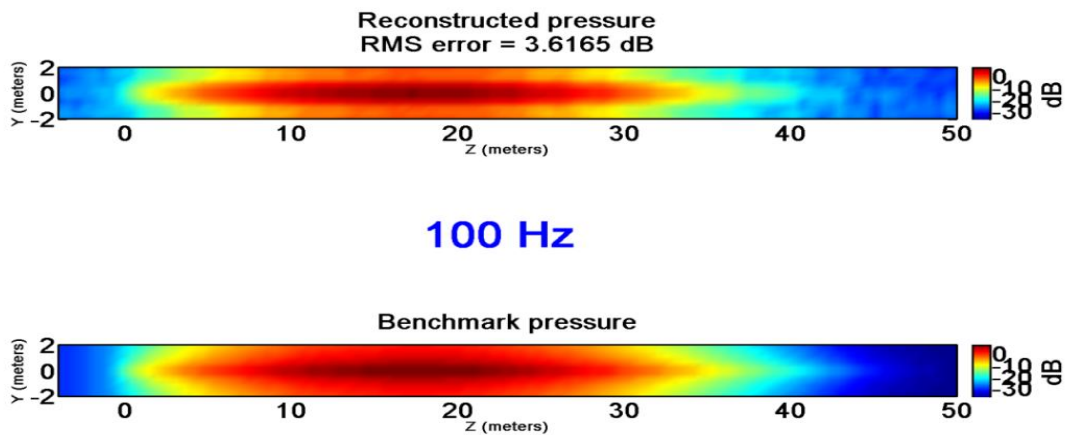


Figure 5 Reconstructed and benchmark pressures (dB) for source at 100 Hz for the linearly spaced reference microphones.



**Figure 6** Top: source locations and reference microphone locations (linearly spaced) in the yz-plane along with the coherence length of the source at 100 Hz at the corresponding z position. Bottom: The dB pressure across the horizontal dimension of the scan at one point in the vertical direction,  $y=0$ m.

Figure 7 compares the reconstructed pressure to the benchmark as before, except now the reference microphones are logarithmically spaced to be more dense where the coherence length is shorter (see Fig. 8). The measured pressure is the same as Fig. 4. Here the RMS error is a little less, at 3.6 dB. This is due to the fact that the denser reference microphones are better able to stitch the field together where it is less coherent towards the nozzle (see Fig. 8 bottom plot).



**Figure 7** Reconstructed and benchmark pressures (dB) for source at 100 Hz for the logarithmically spaced reference microphones.

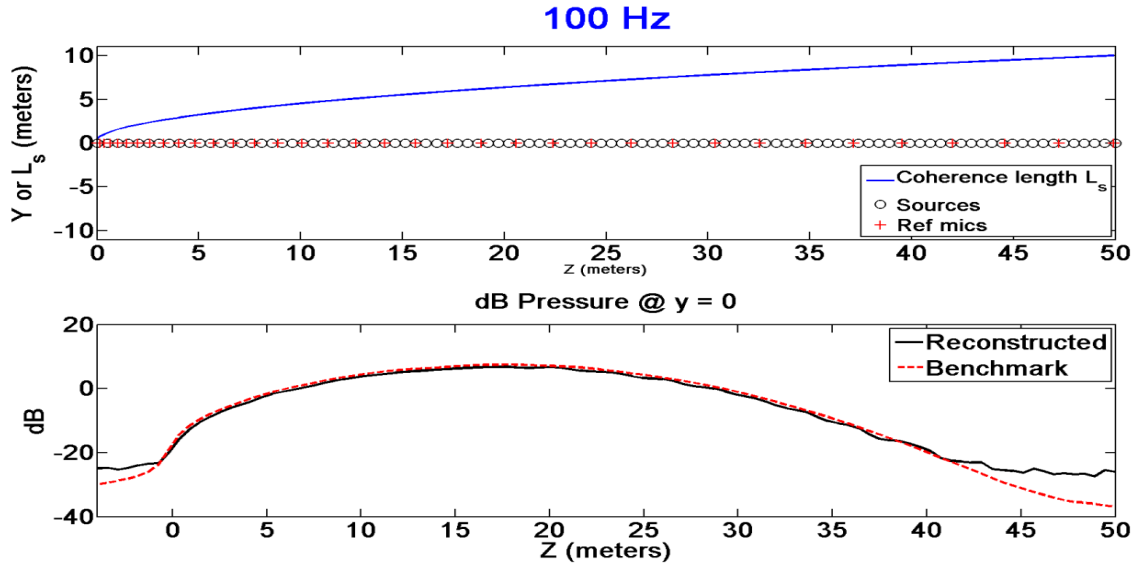


**Figure 8** Top: source locations and reference microphone locations (logarithmically spaced) in the yz-plane along with the coherence length of the source at 100 Hz at the corresponding z position. Bottom: The dB pressure across the horizontal dimension of the scan at one point in the vertical direction,  $y=0\text{m}$

If we now look at the measured pressure for 20 Hz in Fig. 9, we see the hot spot has shifted downstream as is expected for a lower frequency. For the linearly spaced reference microphone array (see Figs. 10 and 11), the RMS error is 1.595 dB. In general, better results are achieved at lower frequencies because the field does not vary as much across the measurement grid.

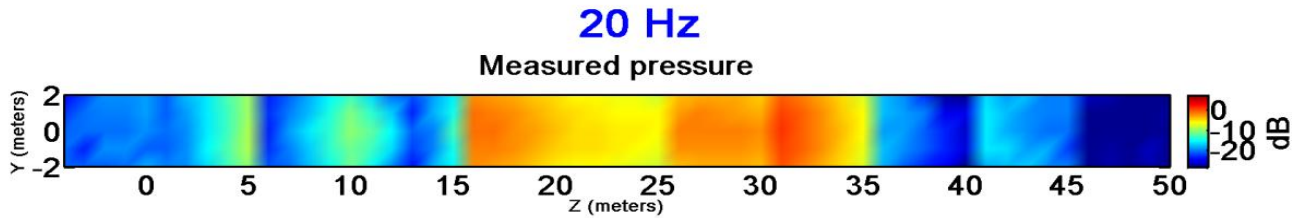


**Figure 9** Measured pressure (dB) at 20 Hz for all the scan positions averaged over blocks



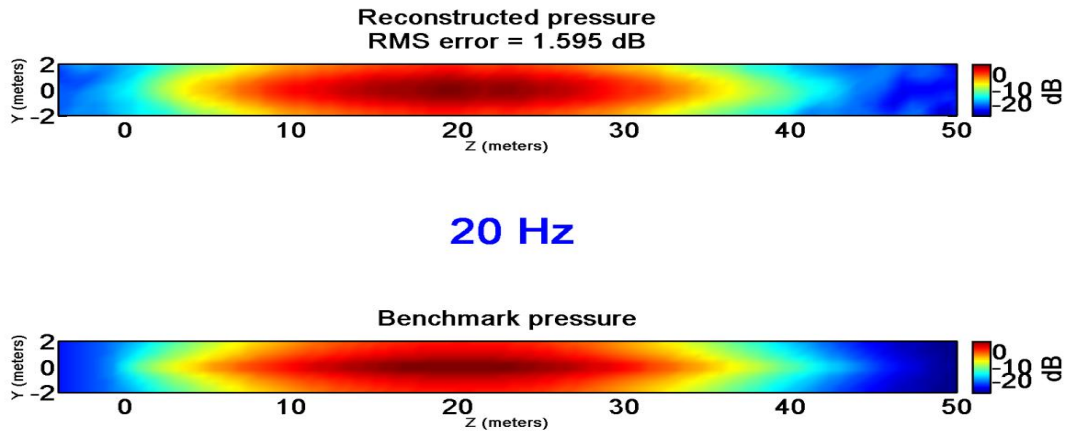


**Figure 10** Reconstructed and benchmark pressures (dB) for source at 20 Hz for the linearly spaced reference microphones.

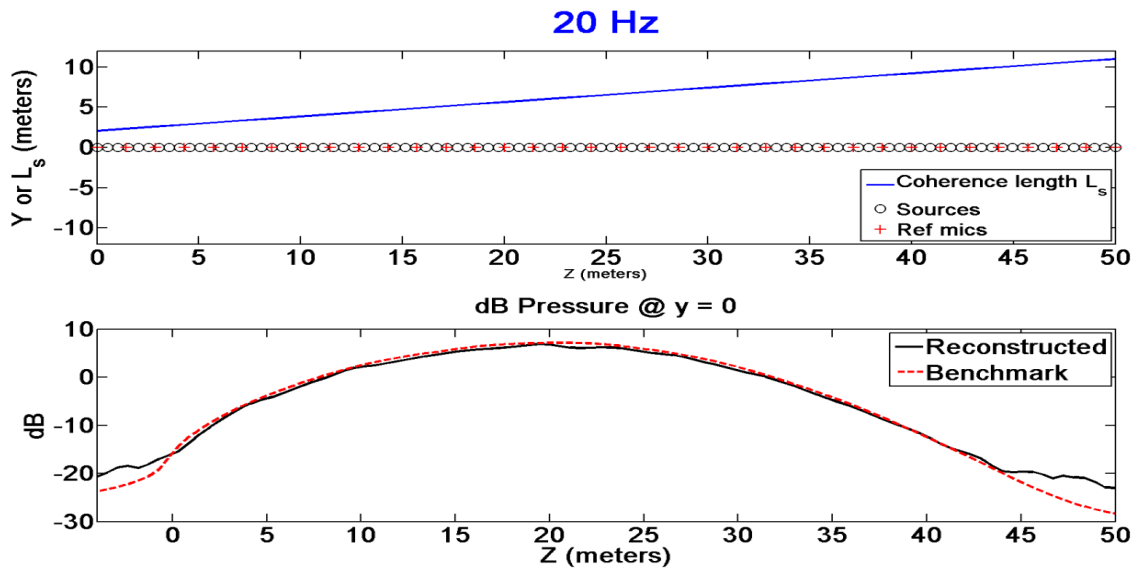


**Figure 11** Top: source locations and reference microphone locations (linearly spaced) in the yz-plane along with the coherence length of the source at 20 Hz at the corresponding z position. Bottom: The dB pressure across the horizontal dimension of the scan at one point in the vertical direction,  $y=0\text{m}$

Taking a look at the results for a logarithmically spaced reference microphone array in Fig. 12, we see the error has actually gone up a little. The uneven spacing is losing too much information downstream where the reference microphones are more widely spaced. We see the reconstructed line departing the benchmark line sooner comparing Fig. 11 (bottom) to Fig. 13 (bottom). The

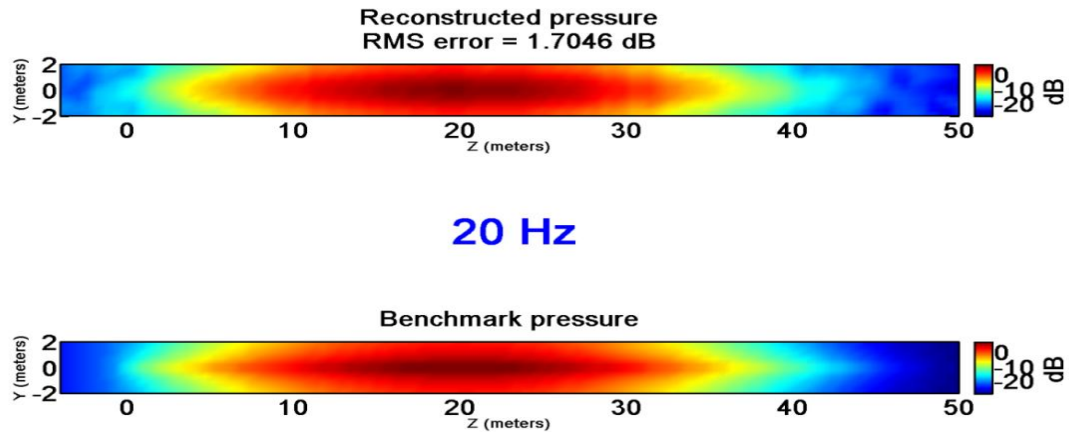


**Figure 12** Reconstructed and benchmark pressures (dB) for source at 20 Hz for the logarithmically spaced reference microphones.

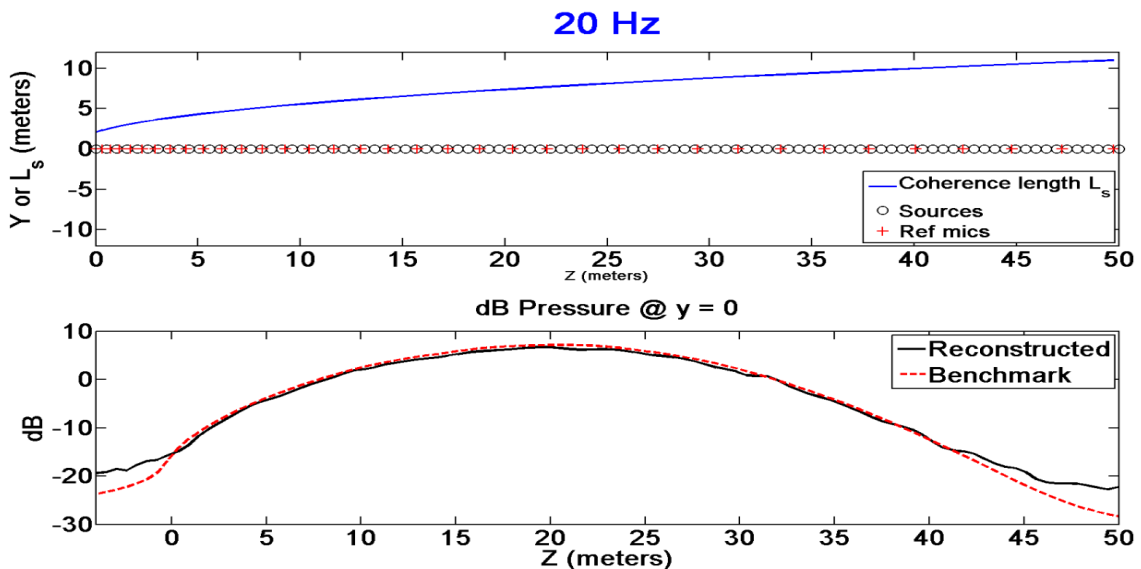


**Figure 13** Top: source locations and reference microphone locations (logarithmically spaced) in the yz-plane along with the coherence length of the source at 20 Hz at the corresponding z position. Bottom: The dB pressure across the horizontal dimension of the scan at one point in the vertical direction,  $y=0m$

overall prediction is very good for both cases and for both frequencies, especially where the source region is.

#### **IV. Discussion/Conclusions**

At 100 Hz, the dB error was 4.2 and 3.6 for linear and logarithmic arrays respectively. For 20 Hz, the error was 1.6 for the linear array and 1.7 for the logarithmic array. What is gained in accuracy from a logarithmically spaced reference microphone array at higher frequencies might be lost at lower frequencies. The reference microphones must be stationary during the entire scan, so whatever spacing is chosen will have to suffice for all frequencies of interest. Therefore, if one is interested in only lower frequency radiation, a linear array might best suit the problem and vice versa for a high frequency study. The more crucial criterion is having enough reference microphones to capture all the field. It should be noted that the models for the frequency dependent spatial amplitude and coherence length were rather simple, and a more complex model may provide more conclusive guidelines. In current rocket noise models, the hot spots for the various frequencies are confined to limited spatial regions; NAH will benefit from this since it performs much better when the amplitude of the source has decayed significantly at the grid boundaries. Rocket noise is thus somewhat self-windowing.

In conclusion, it has been shown that the virtual coherence function when used with SONAH can be a useful tool in characterizing partially correlated sources, like those of a rocket. The greater the number of reference microphones, the better the reconstruction. Guidelines for reference microphone placement are less clear. Having a denser microphone spacing where the coherence length is shorter (higher frequencies) should help reduce error, but it may be it may be detrimental to measuring lower frequencies farther downstream. More research is required to give better guidelines for reference microphone location.

#### **V. Acknowledgments**

I would like to thank the Brigham Young University Department of Physics and Astronomy and Blue Ridge Research and Consulting for their support. I also want to thank my mentor, Dr. Gee, and fellow students, Daniel Manwill and Alan Wall, for their help with the project. I also thank the Rocky Mountain Space Grant Consortium for their support.

<sup>1</sup>T. S. Adams, "Sound power level and directivity pattern determination of a space shuttle solid rocket booster" *J. Acoust. Soc. Am.* 85, S1, pp. S23-S23 (May 1989)

<sup>2</sup>J.D. Maynard, E.G. Williams, and Y. Lee, "Nearfield acoustic holography: I. Theory of generalized holography and the development of NAH," *J. Acoust. Soc. Am.* **78** (4) 1395-1413 (1985)

<sup>3</sup>M. Lee, J.S. Bolton, "Source characterization of a subsonic jet by using near-field acoustical holography," *J. Acoust. Soc. Am.* **121**, 967-977 (2006).

<sup>4</sup>J. Hald, "STSF—A unique technique for scan-based near-field acoustic holography without restrictions on coherence," *B&K Technical Review* No. 1, (1988).

<sup>5</sup>M. Lee, J.S. Bolton, L. Mongeau, "Application of cylindrical near-field acoustical holography to the visualization of aeroacoustic sources," *J. Acoust. Soc. Am.* **114** (2) 842-858 (2003)

<sup>6</sup> M. Lee and J.S. Bolton, "Scan-based near-field acoustical holography and partial field decomposition in the presence of noise and source level variation," *J. Acoust. Soc. Am.*, **119** (1), 382-393 (2006)

<sup>7</sup> R.H. Self, "Jet noise prediction using the Lighthill acoustic analogy," *J. Sound and Vib.* **275** 757-768 (2004)

<sup>8</sup> J. Hald, "Patch near-field acoustical holography using a new statistically optimal method," *Proc. INTER-NOISE 2003*, 2003, 2203-2210.